Journal of Materials Chemistry B

Accepted Manuscript

This article can be cited before page numbers have been issued, to do this please use: B. Shen and Y. Qian, *J. Mater. Chem. B*, 2016, DOI: 10.1039/C6TB02469F.

ROYAL SOCIETY OF CHEMISTRY

www.rsc.org/materialsB

View Article Online
DOI: 10.1039/C6TB02469F

A Novel Triphenylamine-BODIPY Dendrons: Click Synthesis, Near-infrared Emission and Multi-channel Chemodosimeter for Hg^{2+} and Fe^{3+}

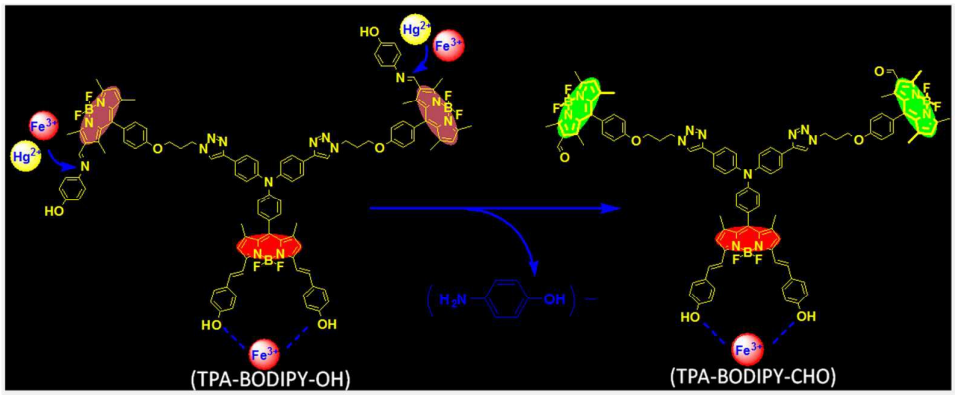

A novel near-infrared emission triphenylamine-BODIPY dendrons for Hg^{2+}, Fe^{3+} detection, fluorescent nanoparticles and living cell imaging.

View Article Online
DOI: 10.1039/C6TB02469F

Journal Name

ARTICLE

A Novel Triphenylamine-BODIPY Dendrons: Click Synthesis, Near-infrared Emission and Multi-channel Chemodosimeter for Hg^{2+} and Fe^{3+}

Received 00th January 20xx,
Accepted 00th January 20xx

DOI: 10.1039/x0xx00000x

www.rsc.org/

Bao-xing Shen and Ying Qian*

A novel triphenylamine-BODIPY based Schiff base fluorescent probe (TPA-BODIPY-OH), with an emission in near-infrared region (NIR) was designed and prepared by click reaction. TPA-BODIPY-OH showed three emission bands at 510 nm, 598 nm and 670 nm, which can detect the Fe^{3+} and Hg^{2+} ions with remarkable fluorescence enhancement in THF/H_2O (v/v, 1:1, buffered with 10 mM HEPES pH=7.4) based on the hydrolysis reaction of -C=N bond, and naked eye detection was realized with the obvious color change. The stoichiometry between probe and ions was deduced from Job's plot showed 1 : 3 for TPA-BODIPY-OH/Fe^{3+} and 1 : 2 for TPA-BODIPY-OH/Hg^{2+}, respectively. Dissociation constant value was found to be 1.35×10^{-16} M for TPA-BODIPY-OH/Fe^{3+} and 2.06×10^{-11} M for TPA-BODIPY-OH/Hg^{2+}. Low detection limit was calculated from titration results with the value were 5.15×10^{-7} M for TPA-BODIPY-OH/Fe^{3+} and 6.81×10^{-7} M for TPA-BODIPY-OH/Hg^{2+}, respectively. In order to investigate the biological applications of TPA-BODIPY-OH, living cell imaging experiment was carried out. The results demonstrate that TPA-BODIPY-OH can be successfully applied as a bioimaging agent in living cells. In addition, amino-group-functionalized silica nanoparticles (Si-NPs) encapsulating the dyes TPA-BODIPY-OH (fluorescent nanoparticles FNPs) was prepared and characterized by transmission electron microscopy. TPA-BODIPY-OH/SiO_2 nanoparticles exhibit good dispersibility, the quantum yield of FNPs at band 657nm was 42.3%.

1. Introduction

In recent years, there has been a tremendous surge in the development of reaction-based molecular probes rather than traditional lock-and-key molecular recognition strategy [1, 2]. These probes undergo target analytes-assisted irreversible chemical reactions, coupled with amplified signal transduction. In most cases, reactive probes display larger spectroscopic changes than traditional chemical probes, owing to the significant structural changes to the molecular probe during the analyte-triggered chemical transformation. In addition, compared with the fluorescence in the visible light range, fluorescent dyes emitting in the near-infrared (NIR) spectral region (650 nm - 900 nm) is gaining momentum [3-8]. Because of the NIR-emitting probes tend to reduce photodamage to biological samples, have deeper tissue penetration, and minimize background fluorescence as well as the environmentally-induced light scattering [9, 10]. Therefore, NIR-emitting fluorescent compounds are of considerable interest in chemical and biological fields [11-14].

Boron dipyrromethene (BODIPY) fluorescent dyes generally have advantageous optical characteristics, such as high extinction coefficients, high fluorescence quantum yields, narrow emission bandwidths and relatively high photostabilities[15-17]. Therefore, BODIPY dyes are considered useful in a variety of research fields [18-22]. On account of the original BODIPY (4, 4-difluoro-4-bora-3a, 4a-diaza-s-indacene) emits at a relatively short wavelength (around 500 nm), various approaches have been presented to obtain NIR-emitting BODIPY derivatives [23]. An efficient way to red-shift the maximum absorption and emission is to extend the conjugated π-system of the BODIPY dyes. So far, the modification reported included the introduction of π-conjugation substituents such as ethyneyl [24, 25], vinyl [26-28] and aromatic groups [29-31] onto the 1, 7- and 3, 5-positions of BODIPY core. On the other hand, multichannel sensors that can show responses towards target analytes have also attracted considerable interest in recent years because of their particularly favorable features such as high sensitivity, selectivity, and convenient visible emission assays due to improved signal-to-noise ratio [32]. It is easy to understand that the detection of multiple targets with single sensor is more efficient and less expensive than a one-to-one analysis method and will attract more and more attention. However, colorimetric and fluorescent sensors which could be used for the multichannel monitoring of different metal ions are rare [33-35].

As we all known, many metal ions have strong influence on biological and environment, especially mercury (Hg^{2+}) and iron ions (Fe^{3+}). Accumulation of mercury in the human body can

School of Chemistry and Chemical Engineering, Southeast University, Nanjing 211189, China. E-mail: yingqian@seu.edu.cn; Fax: +86 25 83795857.

† Footnotes relating to the title and/or authors should appear here.
Electronic Supplementary Information (ESI) available: [details of any supplementary information available should be included here]. See DOI: 10.1039/x0xx00000x

View Article Online
DOI: 10.1039/C6TB02469F

cause a wide variety of diseases such as prenatal brain damage, serious cognitive and motion disorders [36]. Although Fe^{3+} is an essential element in the human body, however high doses of iron ions are dangerous and can be toxic because of their ability to promote oxidation of lipids, proteins and other cellular components [37-40]. Significant effort has been made by scientists toward the development of highly sensitive dosimeters for Hg^{2+} and Fe^{3+}, the majority of them are base on perylene bisimide [41], rhodamine [42], naphthalimide [43] and so on. However, most of them exhibit changes only in fluorescence intensity and the response time is long. What's more, there is only a few reports about fluorescence sensors that can realize the near infrared emission, especially for those probes which can detect various ions based on a same fluorophore are very scarce.

In view of these, on the basis of the unique structure and excellent properties of BODIPY, we fabricate a novel NIR emission fluorescent probe TPA-BODIPY-OH by Cu(I)-catalyzed click reactions (as shown in Scheme 1). It's found that TPA-BODIPY-OH has unique three-channel emissions and can detect the Hg^{2+}, Fe^{3+} ions in complex aqueous samples via different detection modes with C=N functionality and 4-hydroxystyryl groups, which serve as the recognition positions. The near-infrared (NIR) emission was realized by introducing 4-hydroxystyryl group and in conjugation to the 3, 5-positions of triphenylamine-BODIPY core, which is an efficient way to red-shift the maximum absorption and emission band of the BODIPY dyes. TPA-BODIPY-OH was a mixture of reaction-based probe and lock/key-based probe. The BODIPY units of TPA-BODIPY-OH exhibits weak fluorescence due to the nonradiative decay from -C=N isomerization and rotation. When Fe^{3+} or Hg^{2+} ions were added the hydrolysis of Schiff base was promoted by Hg^{2+} and Fe^{3+}, which lead to the -C=N group transform into formyl group and result in considerable fluorescence enhancement in dosimeter TPA-BODIPY-OH. It has high sensitivity for Hg^{2+} and Fe^{3+} ions. Another feature of TPA-BODIPY-OH was the 4-hydroxystyryl groups that conjugate to the 3, 5-positions of BODIPY core, which can bind with Fe^{3+} and enhance the fluorescence of TPA-BODIPY-OH. By introducing the Schiff base and 4-hydroxystyryl groups, the near-infrared emission and multiple recognition based on one fluorescence probe was realized. We further demonstrated that TPA-BODIPY-OH could be used to living cell imaging and exhibited deep red fluorescence in living systems. Moreover, amino-group-functionalized TPA-BODIPY-OH fluorescent nanoparticles were prepared to study the potential application and photophysical properties of it. This method of probe design is an excellent platform for developing near-infrared and multi-channels identification probes.

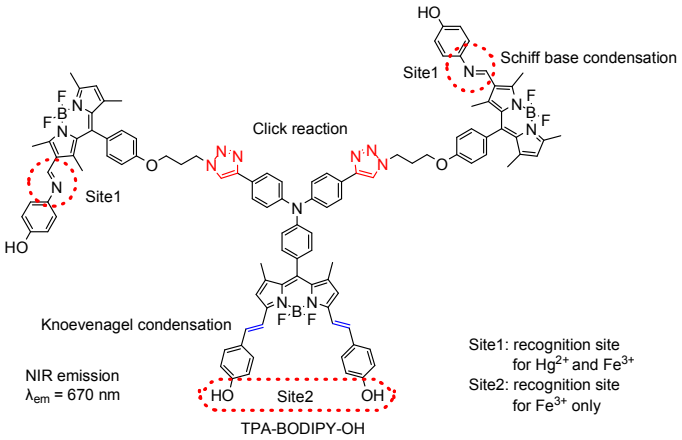

Scheme 1 Structure of R/NIR Chemodosimeter TPA-BODIPY-OH for Hg^{2+} and Fe^{3+}

2. Results and discussion

2.1 Click synthesis of TPA-BODIPY-OH dendrons

The triphenylamine-BODIPY was choosed as the mother fluorophore for the reason of the excellent optical properties that it possessed. The emission band of triphenylamine-BODIPY was about 600 nm, it has been very long even though without any modification. However, we present a triphenylamine-BODIPY based NIR emitting ratiometric fluorophore probe, which was obtained after 3- and 5-positions of triphenylamine-BODIPY fluorophore were substituted with electron-donating 4-hydroxystyryl groups by Knoevenagel condensation. It leads to the emission band of BODIPY unit red shift to the near infrared region. Besides, with the aim of making triphenylamine-BODIPY having broad utility value, the azide substituted Schiff base BODIPY (BODIPY-OH) were added to the maternal fluorophore by Cu(I)-catalyzed click reactions. Interestingly, the BODIPY-OH itself is an excellent multichannel fluorescent sensor. Simply because the functional group of the schiff base, which responded selectively to Hg^{2+} and Fe^{3+} ions through an irreversible -C=N bond hydrolysis reaction. These characteristics were used to develop multi-channel fluorescent chemodosimeters. On top of that, it is well known that phenol oxygen can serve as good ligand donors for metal ions and the phenol group is deprotonated in the coordination process, which can selectively serve as ligand donors for Fe^{3+} ions. Generally speaking, TPA-BODIPY-OH is an excellent platform for developing near-infrared and multi-channels identification probes.

The syntheses of the dendritic probe TPA-BODIPY-OH, intermediate compounds Ey-BODIPY-OH and BODIPY-OH were showed in Scheme 2-4. The intermediate compound Az-BODIPY was prepared according to the standard synthetic procedures of BODIPY [44, 45]. Vilsmeier formylation using DMF-$POCl_3$ gives compound BODIPY-CHO as the sole regioisomer, as this product showed poor stability in air, it was used to the next reaction without further purification. Then, the BODIPY-OH was synthesized by Schiff base condensation, using 4-aminophenol and BODIPY-OH in the presence of ethanol lead

View Article Online
DOI: 10.1039/C6TB02469F

to compound BODIPY-OH in 30% yield. The -C=N is an important group to build multi-channel reaction based probe for Fe^{3+} and Hg^{2+} ions. To obtain the NIR emission fluorophore Ey-BODIPY-OH, p-hydroxy benzaldehyde was conjugated to the 3- and 5-positions of Ey-BODIPY by Knoevenagel condensation. The conjugated π-system of the Ey-BODIPY-OH was extended and the maximum emission band was red-shift to near infrared region. At last, Ey-BODIPY-OH combined with BODIPY-OH by Cu(I)-catalyzed click reaction to produce the TPA-BODIPY-OH dendron.

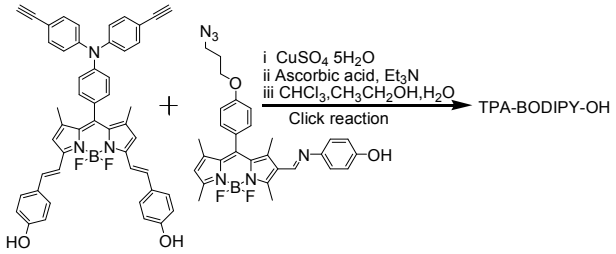

Scheme 2 Synthesis of NIR emission fluorescent dendrons TPA-BODIPY-OH

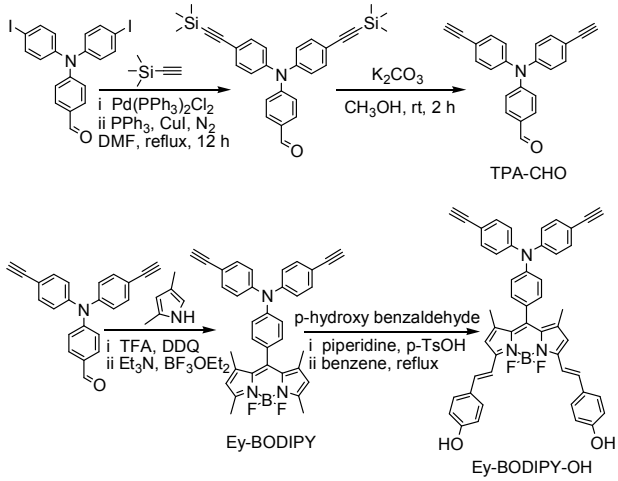

Scheme 3 Synthesis of alkynyl substituted triphenylamine-BODIPY derivatives Ey-BODIPY-OH

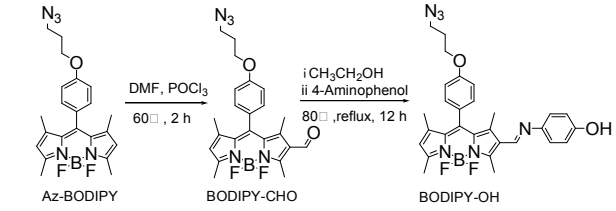

Scheme 4 Synthesis of azide substituted Schiff base BODIPY (BODIPY-OH)

2.2 The sensing behaviour of NIR emission fluorescence probe TPA-BODIPY-OH dendrons

The absorption spectrum and fluorescence spectrum of TPA-BODIPY-OH in H_2O/THF=1:1 was studied by UV/Vis and fluorescence spectroscopy. As shown in Fig. 1a, the UV/Vis spectrum of free TPA-BODIPY-OH (H_2O/THF, 1:1, v/v, buffered with HEPES pH=7.4) displays three maximum absorption band at 494 nm, 587 nm and 650 nm. The absorption peak at band 494 nm belongs to the Schiff base BODIPY (BODIPY-OH), which was added to the triphenylamine-BODIPY by Cu(I)-catalyzed click reactions. The absorption peaks at bands 587 nm and 650 nm belong to mother fluorophore triphenylamine-BODIPY and TPA-BODIPY-OH chromophore respectively. The molar extinction coefficient of absorption peaks at 494 nm, 587 nm and 650 nm was 11.65×10^4/ $cm^{-1} * M^{-1}$, 4.64×10^4/ $cm^{-1} * M^{-1}$, 9.23×10^4/ $cm^{-1} * M^{-1}$ respectively. The fluorescence spectrum of TPA-BODIPY-OH was obtained after excitation within the spectral region of maximal absorption (λ_{ex} = 460 nm, Fig. 1a), which showed three emission bands at 510 nm, 598 nm and 670 nm. Reasonably, TPA-BODIPY-OH was exhibits a very weak emission band at 510 nm, since the molecular structure of the BODIPY derivates bears a C=N functionality that diminishes the emission of the BODIPY core caused by a non-radiative deactivation process involving the rapid isomerization of the C=N group. The fluorescence quantum yield of TPA-BODIPY-OH was measured. In pure THF, the fluorescence quantum yield of TPA-BODIPY-OH at 510 nm was 22.6% relative to fluorescein [46] (Φ_f = 0.95 in 0.1 M NaOH). The quantum yield of TPA-BODIPY-OH at 598 nm and 650 nm were 19.8% and 76.3% respectively, which relative to rhodamine B (Φ_f = 0.31 in H_2O).

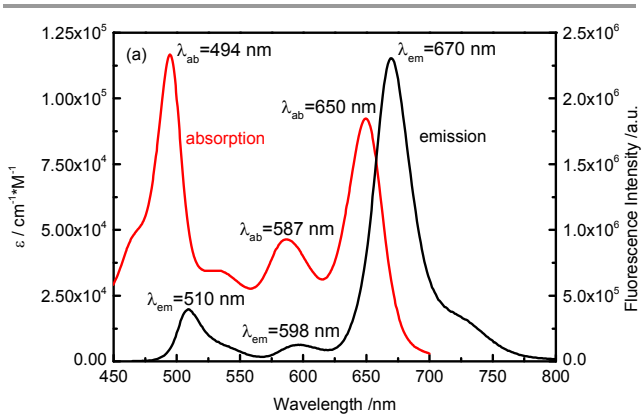

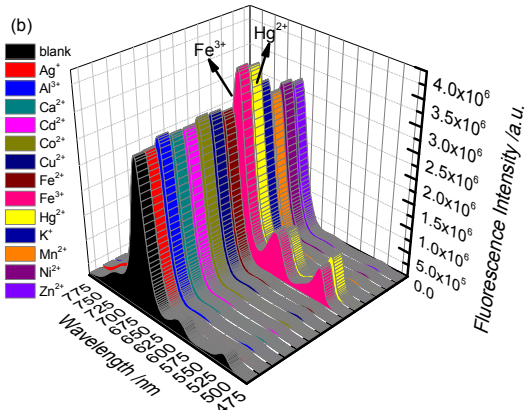

Fig. 1. (a) absorption and fluorescence spectra of TPA-BODIPY-OH in H_2O/THF (1/1, v/v); (b) fluorescence spectra of TPA-BODIPY-OH in the presence of various metal ions in H_2O/THF (1/1, v/v); $C_{TPA\text{-}BODIPY\text{-}OH} = 10^{-5}$ M; $C_{ion} = 5 \times 10^{-5}$ M.

View Article Online
DOI: 10.1039/C6TB02469F

Our investigation began with the evaluation of the optical behaviour of TPA-BODIPY-OH in response to the addition of different ions, such as K^+, Fe^{2+}, Al^{3+}, Ca^{2+}, Mn^{2+}, Co^{2+}, Ni^{2+}, Zn^{2+}, Ag^+, Cd^{2+}, Hg^{2+}, $Fe^{3+}$and Cu^{2+}. The dosimeter showed an intensity emission bands at 510 nm and 670 nm in the buffer solution. No obvious change was obtained, except for Hg^{2+} and Fe^{3+}. The detection of Hg^{2+} and Fe^{3+} by TPA-BODIPY-OH was studied by optical spectroscopy. The addition of Hg^{2+} and Fe^{3+} (5 equiv) to TPA-BODIPY-OH prompted the significant increase of fluorescence intensity at band 510 nm and 670 nm that was assigned to the formation of a new BODIPY derivative (Fig. 1b). The appearance of this spectrum change was accompanied with a distinct change in the solution's emission colour; the purple-emitting probe solution became distinctly green, as was clearly visible to the naked eye (Fig. 2). The emission color photographs of TPA-BODIPY-OH in the presence of Fe^{3+} or Hg^{2+} under excitation at 365 nm was also experience a significant change (Fig. 2). The red fluorescence was enhanced after the addition of Fe^{3+} or Hg^{2+} ions. Table 1 exhibit the photophysical properties of TPA-BODIPY-OH.

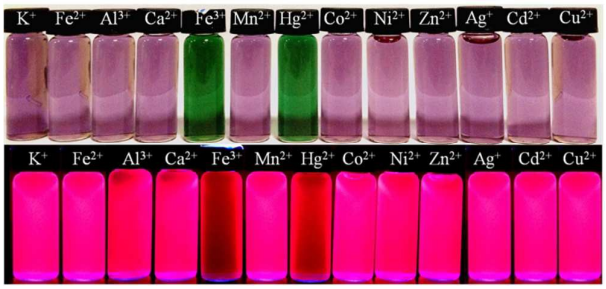

Fig. 2. The corresponding photographs of TPA-BODIPY-OH after the addition metal ions (5.0 equivalent) in H_2O/THF (1/1, v/v, buffered with 10 mM HEPES) using UV lamp at room temperature.

Table1 The molar extinction coefficient, emission band and fluorescence quantum yield of TPA-BODIPY-OH and TPA-BODIPY-OH fluorescent nanoparticles FNPs.

Compounds	λ_{abs} (nm)	ε (10^4 $cm^{-1}*M^{-1}$)	λ_{em} (nm)	Φ_f
	494	11.65	510	0.23
TPA-BODIPY-OH	587	4.64	598	0.19
(H_2O/THF, v/v = 1:1, C=1×10^{-5})	650	9.23	670	0.76
	498	4.77	521	0.10
TPA-BODIPY-OH/ FNPs	590	2.31	605	0.09
(H_2O)	657	1.83	659	0.42

2.3 The fluorescence response to different concentration of Fe^{3+} and Hg^{2+} ions

To further investigate the probe behaviors of TPA-BODIPY-OH towards Fe^{3+} and Hg^{2+} ions, the fluorescence titration experiments of TPA-BODIPY-OH with Fe^{3+} and Hg^{2+} ions were performed in THF/H_2O (1:1, v/v). Fig. 3 showed the fluorescence spectrum changes of TPA-BODIPY-OH as a function of the Fe^{3+} and Hg^{2+} concentration. The titration curve of Fe^{3+} was shown in Fig. 3(a). Notably, the fluorescence intensity at band 510 nm and 670 nm showed a steady increase until a plateau was reached (20 μM Fe^{3+}) with a 3.4-fold and 1.4-fold increase at the plateau, respectively. The fluorescence intensity ratio (F_{510}nm/F_{670}nm) increased over 2.8-fold in presence. Here, there are two important factors that lead to the change of fluorescence spectrum. The one was the structure change of the reaction based probe TPA-BODIPY-OH. Before reaction with the Fe^{3+} and Hg^{2+} ions, the weak fluorescence exhibited at 510 nm due to the nonradiative decay from -C=N isomerization and rotation. After addition of Hg^{2+} ions, the hydrolysis reaction between -C=N and Hg^{2+} ions occured so that -C=N transfer into formyl group, which lead to the enhancement of fluorescence intensity at 510 nm. As for Fe^{3+} ions, the hydrolysis reaction was induced by H^+: Fe^{3+} + H_2O = $Fe(OH)_3$ + $3H^+$. The protons generated by the process reaction of -C=N and the -C=N transfer into formyl group. Therefore, the radiative decay disappeared and fluorescence intensity enhanced. Due to the special structure of TPA-BODIPY-OH, which has two arms extending outward of the fluorophore core just like a antenna. That means after addition of Hg^{2+} or Fe^{3+} ions the fluorescence at 510 nm enhanced and the energy transfer to the whole dendrons and thus lead to the fluorescence enhancement at 670 nm. Meanwhile, the 4-hydroxystyryl group extension at the α-position can also binding with the Fe^{3+} ions, which lead to the increase of fluorescence intensity in the emission spectrum. The fluorescence intensity at 598 nm suffered an increasment with the fluorescence intensity enhanced 2.6-fold at the highest point (15 μM Fe^{3+}).

We made a similar experiment to investigate the TPA-BODIPY-OH in response to different Hg^{2+} concentration. The result was shown in Fig. 3(b). The fluorescence spectrum exhibited the same variation tendency as titration curve of Fe^{3+}. The emission intensities at 510 nm and 670 nm exhibited a drastic change with a 2.8-fold and 1.5-fold increase at the plateau (20 μM Hg^{2+}), respectively, the fluorescence intensity ratio (F_{510nm}/F_{670nm}) increased over 2.4-fold. However, the reason that lead to the enhancement of fluorescence intensity on upon of Hg^{2+} is only the reaction of Hg^{2+} ion and C=N group. The systematic titration of TPA-BODIPY-OH with Fe^{3+} and Hg^{2+} revealed that emission band intensity increases linearly with the increase in concentration of Fe^{3+} or Hg^{2+} in the range of 2.5 - 40 μM (Fig. 3).

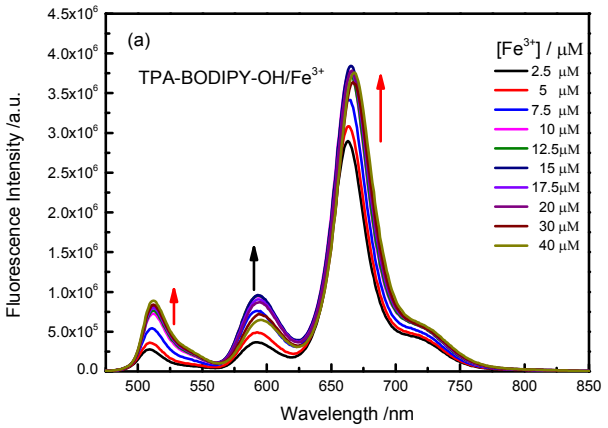

View Article Online
DOI: 10.1039/C6TB02469F

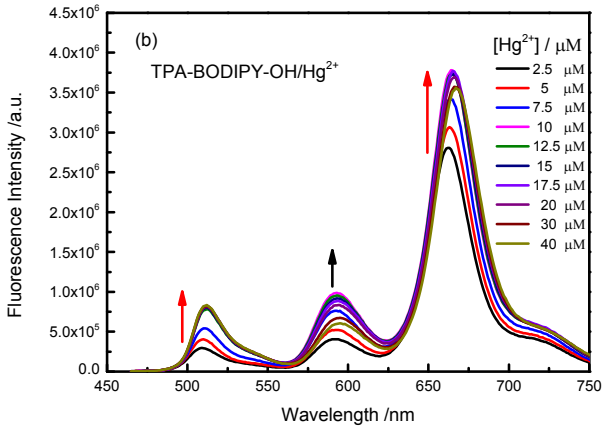

Fig. 3. Fluorescence spectra of TPA-BODIPY-OH with Fe^{3+} (a) and Hg^{2+} (b) in THF/H_2O (1:1, v/v) buffered with 10 mM HEPES, $C_{TPA\text{-}BODIPY\text{-}OH}$ =10^{-5} M.

2.4 Detection of Fe^{3+} and Hg^{2+} ions by TPA-BODIPY-OH

High selectivity toward specific analyst over other competitive species is desired for any sensors, so selectivity and competition experiments were then carried out. Upon addition of 5 equiv of various metal ions aqueous solution (Ag^{+}, Al^{3+}, Ca^{2+}, Cd^{2+}, Co^{2+}, Cu^{2+} Fe^{2+}, Fe^{3+}, Hg^{2+}, K^{+}, Mn^{2+}, Ni^{2+}, and Zn^{2+}) to TPA-BODIPY-OH in THF/H_2O (1:1, v/v) system, probe TPA-BODIPY-OH displayed significantly enhanced fluorescence effects in the presence of Fe^{3+}, Hg^{2+} and almost no obvious fluorescence changes from Ag^{+}, Al^{3+}, Ca^{2+}, Cd^{2+}, Co^{2+}, Cu^{2+} Fe^{2+}, K^{+}, Mn^{2+}, Ni^{2+}, and Zn^{2+}. As show in Fig.4a-b, the fluorescence response to the addition of Fe^{3+} and Hg^{2+} was hardly affected by the presence of these commonly coexistent ions, indicating the exclusive sensitivity of TPA-BODIPY-OH toward Fe^{3+} and Hg^{2+}. The probe behaviour of the probe towards the Fe^{3+} and Hg^{2+} can be attributed to the reaction of the C=N group. Meanwhile, the 4-hydroxystyryl group extension at the α-position can also binding with the Fe^{3+} ions, which is different from Hg^{2+}.

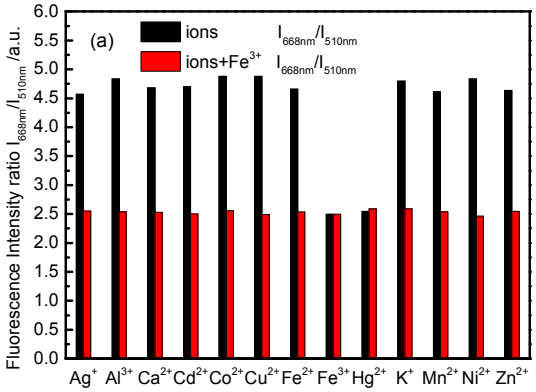

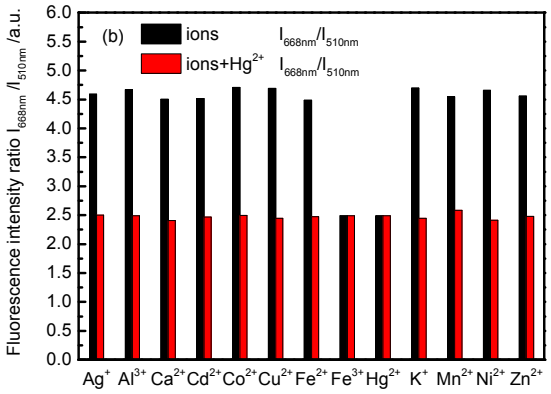

Fig. 4. Fluorescence responses of TPA-BODIPY-OH to various cations in THF/H_2O (1:1, v/v) system buffered with HEPES. ($C_{TPA\text{-}BODIPY\text{-}OH}$=10 μM; C_{ion}= 50 μM). The high bars represent the addition of Ag^{+}, Al^{3+}, Ca^{2+}, Cd^{2+}, Co^{2+}, Cu^{2+}, Fe^{2+}, Fe^{3+}, Hg^{2+}, K^{+}, Mn^{2+}, Ni^{2+}, and Zn^{2+} ions to the solution of TPA-BODIPY-OH, respectively. The short bars represent the subsequent addition of Fe^{3+} or Hg^{2+} to the solution. (λ_{ex} = 450 nm).

2.5 Dissociation constant and the detection limit of probe TPA-BODIPY-OH

For determination of stoichiometry between TPA-BODIPY-OH with Fe^{3+} or Hg^{2+}, Job's plot analyses were used. The method is that keeping total concentration of TPA-BODIPY-OH and Fe^{3+} (or Hg^{2+}) at 10^{-4} M, and changing the molar ratio of ions (X_{ion}; X_{ion} = [ion] / ([probe] + [ion])) from 0.1 to 0.9. The result was shown in Fig. 5(a-b), when molar fraction of Fe^{3+} was 0.73, the fitting curve of job's plot for Fe^{3+} reach the highest point, indicating the stoichiometry between TPA-BODIPY-OH and Fe^{3+} was 1:3. The similar experiment was measured for Hg^{2+} and the corresponding result was shown in Fig. 5(b). The highest point was found in the fitting curve with the molar ratio of Hg^{2+} ions at 0.65, which means the stoichiometry between TPA-BODIPY-OH and Hg^{2+} was 1:2.

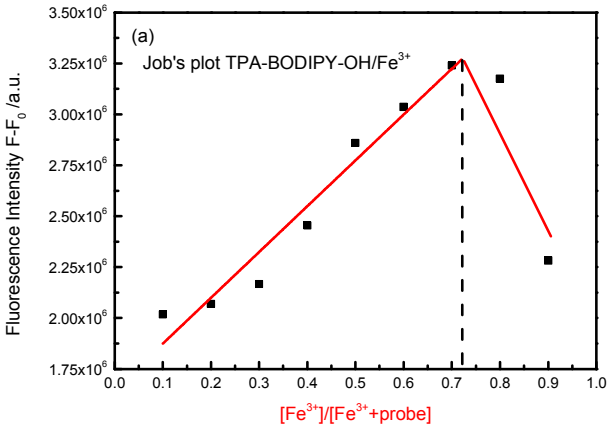

View Article Online
DOI: 10.1039/C6TB02469F

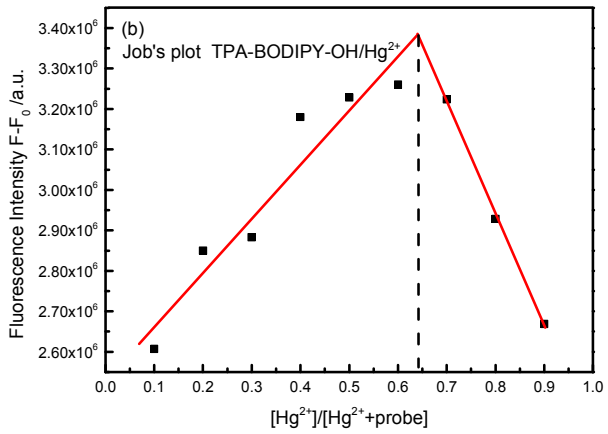

Fig. 5. (a) Job's plot of TPA-BODIPY-OH with Fe^{3+}; (b) Job's plot of TPA-BODIPY-OH with Hg^{2+}; THF/H_2O = 1:1 buffered with HEPES (pH=7.4); the total concentration of [probe] + [ion] was kept constant at 100 μM (λ_{ex}= 450 nm).

The apparent dissociation constant (K_d) was obtained by direct fluorometric titration as a function of Fe^{3+} and Hg^{2+} using the fluorescence emission spectra according to the reported method [47, 48]. The fluorescence intensity data (Fig. 3) was fitted to equation: $F=(F_{min}K_d + F_{max}[X]^n)/(K_d + [X]^n)$; F_{min} and F_{max} are the fluorescence intensities with no addition of ion and excess amount of ion at 670 nm, respectively; n is the binding stoichiometry between TPA-BODIPY-OH and Fe^{3+} or Hg^{2+}; [X] is the concentration of ions added. The stoichiometry between probe and Fe^{3+} or Hg^{2+} were kept fixed at 3 or 2 in the final curve fittings, accordingly, the related dissociation constant value was found to be 1.35×10^{-16} M for TPA-BODIPY-OH/Fe^{3+} and 2.06×10^{-11} M for TPA-BODIPY-OH/Hg^{2+}. The detection limit was measured to be 5.15×10^{-7} M for TPA-BODIPY-OH/Fe^{3+} (3s/slope, s is the standard deviation of the blank measurement)[49] and 6.81×10^{-7} M for TPA-BODIPY-OH/Hg^{2+}, respectively. Compared with the similar probes that have been reported, the results of dissociation constant and detection limit for TPA-BODIPY-OH are better than it.

2. 6 Sensing modes based on Schiff base hydrolysis reaction and Fe^{3+} ion binding

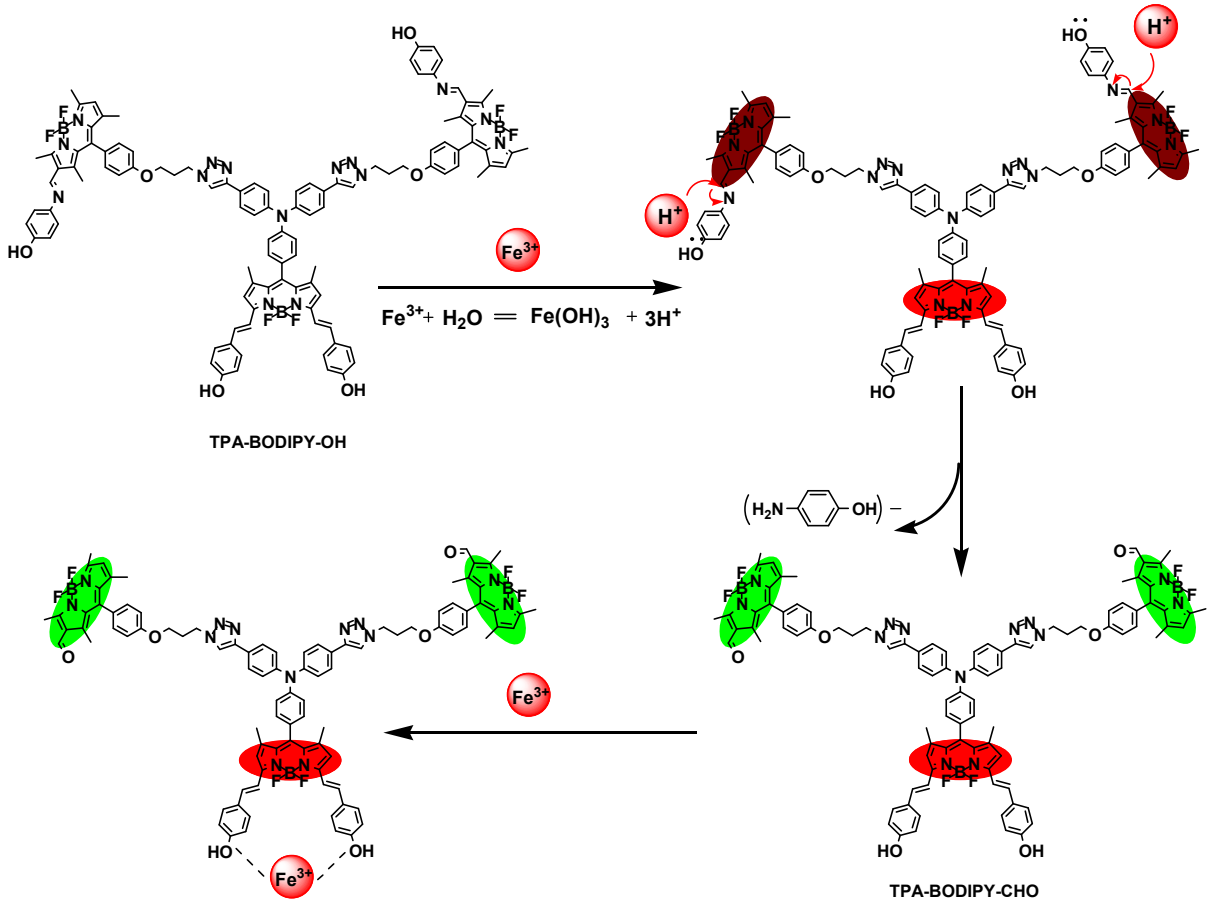

Fig. 6. The possible mechanism of TPA-BODIPY-OH toward Fe^{3+} ions in THF/H_2O (1:1, v/v) system buffered with HEPES.

View Article Online
DOI: 10.1039/C6TB02469F

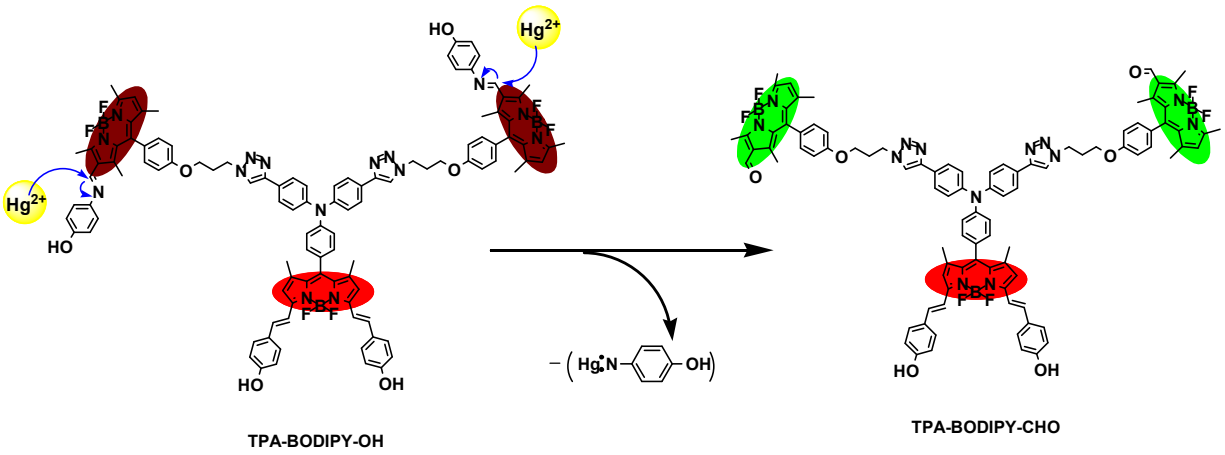

Fig. 7. The possible mechanism of TPA-BODIPY-OH toward Hg^{2+} ions in THF/H_2O (1:1, v/v) system buffered with HEPES

As we discussed above, the dosimeter TPA-BODIPY-OH displayed an unchanged fluorescence emission in THF/H_2O solution on addition of Ag^+, Al^{3+}, Ca^{2+}, Cd^{2+}, Co^{2+}, Cu^{2+}, Fe^{2+}, K^+, Mn^{2+}, Ni^{2+}, and Zn^{2+}, but when $Hg^{2+}$and Fe^{3+} ions was added, it showed obvious enhancement of fluorescence intensity at band 510 nm and 670 nm. There are two reasons, the first one is that the change of molecular structure. The -C=N functionality diminishes the emission of the BODIPY core at band 510 nm caused by a non-radiative deactivation process involving the isomerization of the -C=N group. However, after Hg^{2+} and Fe^{3+} ions were added, an irreversible C=N bond hydrolysis reaction occurred (as shown in Fig. 6 and Fig. 7), at the same time the -C=N transfer into formyl group. Therefore, the radiative decay disappeared and fluorescence intensity enhanced at band 510 nm. However, the hydrolysis reaction of -C=N with Fe^{3+} ions in aqueous solution was induced by H^+: $Fe^{3+} + H_2O = Fe(OH)_3 + 3H^+$. By reason of the special structure of TPA-BODIPY-OH, which has two arms extending outward of the fluorophore core just like a slight antenna. So after addition of Hg^{2+} or Fe^{3+} ions the fluorescence at 510 nm enhanced and the energy transfer to the whole dendrons and thus lead to the fluorescence enhancement at 670 nm. On the other hand, the Fe^{3+} ions can also coordination with the phenolic hydroxyl like 4-hydroxystyryl group, which was in conjugation to the 3- and 5-positions of triphenylamine-BODIPY core. The Fe^{3+} formed complexes with TPA-BODIPY-CHO (as shown in Fig. 6) via coordination with the 4-hydroxystyryl moiety. It should be noted that the TPA-BODIPY-CHO/Fe^{3+} complex partially retained the monoanion character. The existing negative charge in TPA-BODIPYCHO/Fe^{3+} resisted the deprotonation of the second phenolic proton (Ph-OH → PhO^-), as this required the formation of a dianion with the higher energy, the result was reference to the reported literature [50]. The binding of Fe^{3+} with the lone pair on the oxygen atom in TPA-BODIPY-CHO lead to an increase of delocalization extent of mother fluorophore triphenylamine-BODIPY. This result in the enhancement of the fluorescence intensity at band 670 nm.

To confirm the hydrolysis reaction of -C=N with ions, the mass spectrum was carried out. The formation of BODIPY-OH and Fe^{3+} mixture upon addition of 5 equiv of Fe^{3+} to a solution of BODIPY-OH. As shown in Fig. 8, the peaks of key intermediate compound $[BODIPY\text{-}OH]^+$ (m/z = 543.2491) was obtained. After reaction with Fe^{3+}, the -C=N group turn into -C=O and the BODIPY-OH changed into BODIPY-CHO. The peaks of ionic fragments $[BODIPY\text{-}CHO]^+$ (m/z = 452.2069) and $[BODIPY\text{-}CHO]+Na^+$ (m/z = 474.1889) was founded in the mass spectrum. The results proved that the reactions between -C=N and Fe^{3+} have took place.

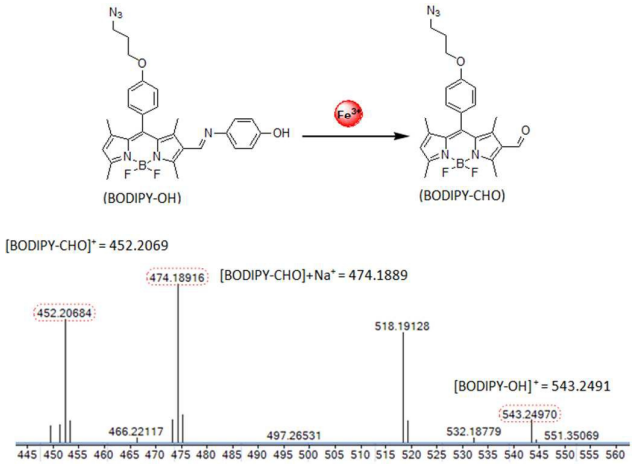

Fig. 8. Mass spectrum of Schiff base BODIPY (BODIPY-OH) with Fe^{3+}.

2.7 Preparation of functionalized fluorescent core-shell nanoparticles

View Article Online
DOI: 10.1039/C6TB02469F

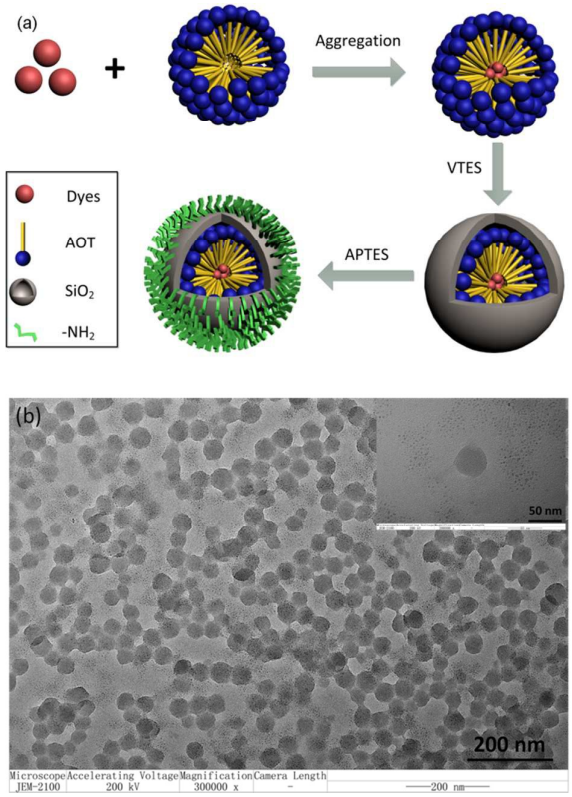

Fig. 9. (a) The preparation process and model structure of TPA-BODIPY-OH fluorescent nanoparticles FNPs; (b) The TEM image of TPA-BODIPY-OH fluorescent nanoparticles.

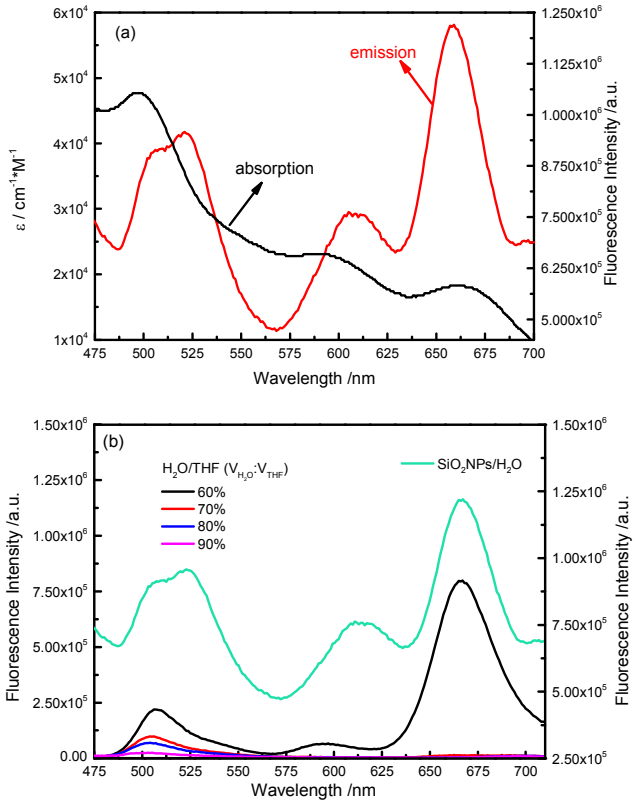

Fig. 10. (a) Absorption and fluorescence spectrums of TPA-BODIPY-OH fluorescent nanoparticles; (b) Fluorescence spectrum of TPA-BODIPY-OH fluorescent nanoparticles and TPA-BODIPY-OH in THF/H_2O system with different water fraction. (C=10^{-5} M, λ_{ex}= 460 nm).

The amino-modified TPA-BODIPY-OH fluorescent nanoparticles FNPs were synthesized using the oil /water (O/W) micelle microemulsion method and the preparation process are shown in Fig. 9(a). The model structure of the FNPs is presented in Fig. 9. It consists of two parts: (1) the core made of aggregated chromophore molecules; (2) the silica shell whose internal surface was modified by vinyl, which would create a non-polar environment for organic chromophores, while the outside surface was decorated with amino groups, which would provide bonding sites for biomolecules. These nanoparticles were characterized by transmission electron microscopy. The results showed that the particle sizes of TPA-BODIPY-OH fluorescent nanoparticles FNPs were about 50 ± 5 nm (Fig. 9(b)), and the particles were spheric and dispersed in water. This property was conducive to the easy uptake of FNPs by living cells. In addition, the fluorescence spectrum of TPA-BODIPY-OH fluorescent nanoparticle was characterized by a fluorometer. The FNPs can be well dispersed in water while the good inherent photophysical properties of the pure dyes were maintained, as presented in Fig. 10(a). The absorption peaks of dye-doped FNPs were at 500, 588, and 658 nm, whereas the emission peaks were at 520, 605, and 660 nm. The fluorescence spectrum of the nanoparticles indicating that the spectral characterization of the TPA-BODIPY-OH dye did not change to a great extent when it was doped inside the nanoparticles.

To further investigate the fluorescence properties of the TPA-BODIPY-OH fluorescent nanoparticles, the emission spectrum of TPA-BODIPY-OH fluorescent nanoparticle was compared with TPA-BODIPY-OH in mixed solvent of water and THF system with different water fraction, as shown in Fig. 10(b). It was obvious that the emission peaks of dyes encapsulated inside the silica shell were similar to those in mixed solvent of water and THF system with low water fraction, and different from those in mix-solvents with high water fractions such as 70%, 80% and 90%. Moreover, the fluorescence intensity of TPA-BODIPY-OH fluorescent nanoparticle was higher than the TPA-BODIPY-OH in mixed solvent of water and THF system with water fraction over 60%. What's moer, the quantum yield of TPA-BODIPY-OH fluorescent nanoparticles at band 660 nm was up to 42.3%. Thus, it could be concluded that the excellent photophysical properties of the TPA-BODIPY-OH was maintained in the Si-NPs. However, the potential bioapplications based on the Si-NPs still need to be further researched[51-54].

2.8 Live cell imaging

To demonstrate the potential application of them in the biological systems, the utility of probe TPA-BODIPY-OH in living cells was studied. A549 cells were cultured on confocal dishs at 1.6×10^4/dish at 37 ℃ under 5 % CO_2 for 24 h. Then the cells were cultured in 10 μL 10^{-6} mol TPA-BODIPY-OH at 37 ℃

View Article Online
DOI: 10.1039/C6TB02469F

containing 100 μL cell PBS for 30 min. Afterward, cells were washed with PBS for three times to remove the nonspecifically absorbed dyes. Cell imaging was performed using a laser-scanning confocal fluorescent microscope (leica, TCS-SP8) with an excitation wavelength of 405 nm. The A549 cells stained by TPA-BODIPY-OH displayed a strong fluorescence in different channels as shown in Fig. 11a-d. The cells displayed bright green fluorescence in green field. What's more if the emissions windows were set at yellow-green field or red field, the cells can also display yellow-green or red fluorescence, respectively. These preliminary results indicate the good photostability of the TPA-BODIPY-OH in a biological environment.

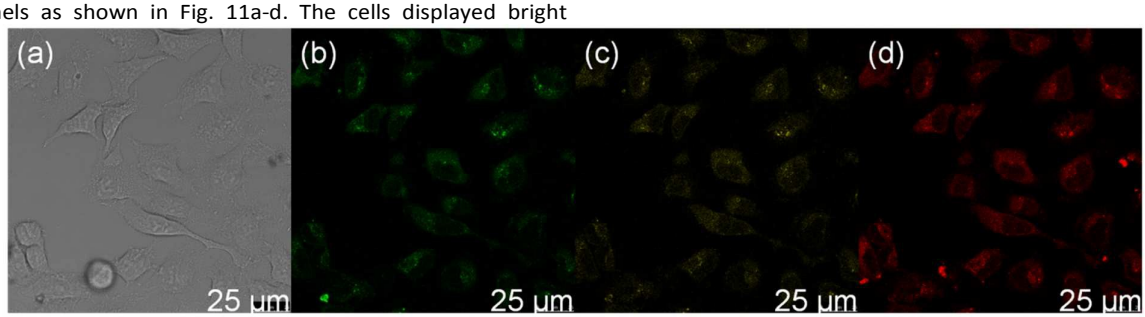

Fig. 11. Fluorescence images of A549 cells incubated with TPA-BODIPY-OH (10 μL, 1 μM) for 30 min. (a) fluorescence image of A549 cells in brightfield; (b) fluorescence image of (a) in the green channel; (c) fluorescence image of (a) in the yellow-green channel; (d) fluorescence image of (a) in the red channel.

3. Conclusions

In summary, a novel near-infrared region emitting fluorescent probe TPA-BODIPY-OH was synthesised by click reaction. The TPA-BODIPY-OH showed excellent sensitivity for fluorescent determination of Hg^{2+} and Fe^{3+} ions based on Schiff base hydrolysis reaction. Especially for Fe^{3+} ions, which can realize the multi-channel detection by -C=N bond and 4-hydroxystyryl group. "Naked eye" detection was realized with the obvious colour change from purple-emitting to distinctly green. The stoichiometry between TPA-BODIPY-OH and ions was deduced from Job's plot showed 1:3 for TPA-BODIPY-OH/Fe^{3+} and 1:2 for TPA-BODIPY-OH/Hg^{2+}, respectively. Dissociation constant value was found to be 1.35×10^{-16} M for TPA-BODIPY-OH/Fe^{3+} and 2.06×10^{-11} M for TPA-BODIPY-OH/Hg^{2+}. Besides, low detection limit was calculated from titration results with the value were 5.15×10^{-7} M for TPA-BODIPY-OH/Fe^{3+} and 6.81×10^{-7} M for TPA-BODIPY-OH/Hg^{2+}, respectively. Furthermore, the TEM image showed that the sizes of TPA-BODIPY-OH/SiO_2 nanoparticles were about 50 ± 5 nm, and the nanoparticles exhibit excellent dispersibility and photophysical properties, which indicate that TPA-BODIPY-OH has a great application potential in ions detection and biomedical field. Cell imaging experiment was successfully carried out and the A549 cells displayed a bright red fluorescence. This novel molecular structure will have great significance to help develop near-infrared emission fluorescence probes with other specific natures by click reaction.

4. Experimental

4.1 Materials and methods

^1H NMR and ^{13}C NMR spectra were recorded on a Bruker DMX 300 NMR spectrometer in $CDCl_3$ with tetramethylsilane (TMS) as internal standard. Chemical shifts are given in parts per million (ppm). Mass spectra were recorded on Agilent Technologies 6530 Accurate-Mass Q-TOF LC/MS. All reagents used were purchased from Aldrich, Fluka or Alfa Aesar and used without further purification. All solvents used in spectroscopic measurements were of analytical grade. 3-Aminopropyltriethoxysilane (APTES, Sinopharm Chemical Reagent Co., Ltd, Shanghai, China), Aerosol OT (AOT, Aladdin Industrial Co., Shanghai, China), triethoxyvinylsilane (VTES, Aladdin Industrial Co., Shanghai, China) were also used. Reactions were monitored by thin layer chromatography using Merck TLC Silica gel 60 F254. Silica gel column chromatography was performed over Merck Silica gel 60. UV-visible absorption spectra were determined on a Shimadzu UV-3600 spectrophotometer. Fluorescence spectra were measured on a HORIBA FL-4 Max spectrometer. The absorption and fluorescence spectral titrations of dosimeter TPA-BODIPY-OH were prepared in THF-H_2O, the solutions of guest cations were prepared in H_2O in the order of 10^{-6} M. Absorption and fluorescence spectra were recorded after mixing dosimeter TPA-BODIPY-OH with metal ions like K^+, Na^+, Al^{3+}, Ca^{2+}, Mn^{2+}, Fe^{2+}, Co^{2+}, Ni^{2+}, Zn^{2+}, Ag^+, Cd^{2+}, Hg^{2+}, and Cu^{2+}. Cell imaging was performed using a laser-scanning confocal fluorescent microscope (leica, TCS-SP8) with an excitation wavelength of 488 nm.

4.2 Synthesis

The synthetic routes adopted for preparation of TPA-BODIPY-OH were shown in Scheme 2-4. The detailed synthesis methods of compound TPA-CHO, Az-BODIPY and compound 2,4-dimethyl pyrrole were in the supporting information.

Compound Ey-BODIPY: 2,4-dimethyl pyrrole (2.01g, 21 mmol) and compound TPA-CHO (3.36 g, 10.47 mmol) were dissolved in dry dichloromethane (200 mL). Three drop of trifluoroacetic acid (TFA) was added to the solution. The reaction mixture was stirred at room temperature for 24 h. The reaction was monitored by TCL. After disappearance of the aldehyde, a solution of p-chloranil (2.57 g, 10.47 mmol) in

View Article Online
DOI: 10.1039/C6TB02469F

dichloromethane was added. The reaction mixture was stirred at room temperature for 12 h. Absolute triethylamine (15 mL) was then added to the mixture. At last $BF_3.OEt_2$ (15 mL) was added dropwise at 0℃. The mixture was stirred 12 h again and then the reaction mixture was washed with water for three times (100×3 mL) and extracted with dichloromethane. The organic layer was dried over Na_2SO_4. The solvent was evaporated and the residue was purified by silica gel column chromatography using dichloromethane as eluent to obtain a yellow solid 0.5 g, yield: 8.86 %. ^{1}H NMR ($CDCl_3$, ppm, 300 MHz) δ: 7.44 (d, *J*=9.0 Hz 4H), 7.21 (s, 4H), 7.05 (d, *J*=9.0 Hz, 4H), 6.03 (s, 2H), 3.22 (d, *J*=6.0 Hz, 2H), 2.57 (s, 6H), 1.58 (s, 6H). ^{13}C NMR ($CDCl_3$, ppm) δ: 155.48, 147.13, 142.78, 133.40, 130.07, 129.34, 124.97, 123.68, 121.29, 116.83, 83.31, 77.45, 77.00, 76.60, 58. 24, 46.76, 18.28, 14.47, 8.60.

Compound Ey-BODIPY-OH: In a 50 mL round-bottomed flask equipped with a Dean-Stark trap and a reflux condenser were added 20 mL benzene, Ey-BODIPY (0.10 g, 0.19 mmol, 1.0 eq.), p-hydroxybenzaldehyde (48 mg, 0.40 mmol, 2.1 eq.), one spatula of p-TsOH, and piperidine (0.5 mL). The reaction mixture was stirred overnight at reflux under N_2 atmosphere. After cooling to room temperature, water was added to the reaction mixture, it was extracted three times with CH_2Cl_2. The organic phase was washed with brine and dried over anhydrous Na_2SO_4. The solvent was evaporated and the residue was purified by silica gel column chromatography (DCM: PE: methanol = 10 : 10 : 1). Ey-BODIPY-OH was obtained as blue-purple solid (71 mg, 50 %). ^{1}H NMR ($CDCl_3$, ppm, 300 MHz) δ: 7.61 (s, 1H), 7.56 (d, 1H), 7.51 (d, J=9.0 Hz, 4H), 7.43 (d, J=9.0 Hz, 4H), 7.26 (s, 4H), 7.22 (s, 4H), 7.04 (d, J=6.0 Hz, 4H), 6.86 (d, J=6.0 Hz, 4H), 6.64 (s, 2H), 3.07 (s, 2H), 1.62 (s, 3H), 1.26 (s, 3H). ^{13}C NMR ($CDCl_3$, ppm) δ: 157.24, 152.75, 147.19, 141.38, 136.04, 133.41, 129.94, 129.20, 124.94, 123.65, 117.58, 116.87, 115.83, 83.35, 77.40, 76.97, 76.55, 58.41, 29.64, 18.34, 14.74.

Compound BODIPY-CHO: A mixture of DMF (6 mL) and $POCl_3$ (6 mL) was stirred in an ice bath for 30 min. After removing the ice bath and warming to room temperature, N_3-BODIPY (0.50 g, 1.18 mmol) in 1, 2-dichloroethane (30 mL) was added, which was then heated for 2 h at 50 ℃. When the reaction mixture was cooled to room temperature, it was slowly poured into a saturated $NaHCO_3$ aqueous solution (100 mL) with an ice bath. The mixture was warmed to room temperature, further stirred for 30 min, and washed with water twice (50×3 mL). The organic layer was separated and dried over anhydrous Na_2SO_4. Then the solvent was evaporated in vacuo. Account for the instability of BODIPY-CHO, the crude product was used in the next reaction without purification.

Compound BODIPY-OH: A mixture of compound BODIPY-CHO (0.50 g, 1.1 mmol) and 4-aminophenol (0.16 g, 1.46 mmol) in ethanol (30 mL) was heated at 80 ℃ for 12 h. After the reaction was completed, the mixture was poured into water (50 mL) and extracted with dichloromethane (100 mL×3), the organic phase was dried over Na_2SO_4. The solvent was evaporated and the residue was purified by silica gel column chromatography (CH_2Cl_2/methanol, 9:1). A purple solid got 0.18 g, yield: 30%. ^{1}H NMR ($CDCl_3$, ppm, 300 MHz) δ: 8.45 (s, 1H), 7.23 (d, J=6.0 Hz, 2H), 7.08 (d, J=6.0 Hz, 4H), 6.86 (d, J=6.0 Hz, 2H), 6.10 (s, 1H), 4.16 (t, J =6.0 Hz, 2H), 3.60 (t, J =6.0 Hz, 2H), 2.91 (s, 3H), 2.63 (s, 3H), 2.14 (q, J =6.0 Hz, 2H), 1.73 (s, 3H), 1.49 (s, 3H). ^{13}C NMR ($CDCl_3$, ppm) δ: 159.43, 151.85, 129.06, 127.02, 122.39, 121.84, 116.07, 115.82, 115.50, 115.37, 115.21, 77.43, 77.01, 76.58, 64.68, 58.26, 48.16, 45.86, 29.62, 28.72, 18.25, 15.03, 14.79, 13.87, 12.37.

Compound TPA-BODIPY-OH: A solution of compound BODIPY-OH (0.15 g, 0.27 mmol), Ey-BODIPY-OH (0.1 g, 0.13 mmol), sodium ascorbate (0.0028 g, 0.014 mmol), and cupric sulfate (0.0035 g, 0.014 mmol) in a mixture of chloroform, ethanol and water (v/v/v = 12 : 3 : 2) was stirred at room temperature for 48 h. After completion of the reaction, the solvents were removed under reduced pressure and the crude product was purified by column chromatography (CH_2Cl_2 / methanol=10 : 1). A purple solid was obtained 0.11 g, yield: 50 %. ^{1}H NMR ($CDCl_3$, ppm, 300 MHz) δ: 9.97 (d, J=9.0 Hz 2H), 9.38 (s, 2H), 8.55 (d, J =24.0 Hz, 4H), 7.81 (s, 4H), 7.49 (d, J=6.0 Hz, 5H), 7.38 (s, 2H), 7.30 (d, J=6.0 Hz, 7H), 7.15 (m, 11H), 7.09 (d, J=9.0Hz, 4H), 6.90 (t, J1=12.0 Hz J2=9.0 Hz, 5H), 6.76 (d, J=9.0Hz, 2H), 6.26 (s, 4H), 4.63 (s, 4H), 4.11 (s, 4H), 2.78 (d, J=27.0 Hz, 4H), 2.50 (s, 6H), 2.39 (s, 6H), 1.66 (d, J=12.0 Hz, 6H), 1.41 (s, 6H), 1.23 (d, J=18.0 Hz, 6H). ^{13}C NMR ($CDCl_3$, ppm) δ: 186.02, 150.21, 144.91, 143.42, 136.61, 129.16, 126.85, 124.51, 116.01, 115.35, 109.15, 77.43, 77.00, 76.58, 71.97, 67.89, 66.35, 64.39, 58.19, 45.88, 29.61, 29.24, 18.26, 15.02, 11.73, 8.51.

4.3 Preparation of dye-encapsulated amine-functionalized silica nanoparticles

To a clear solution of surfactant AOT (0.44 g) dissolved in deionized water (20 mL), 0.8 mL of co-surfactant 1-butanol was added with sonication at 0 ℃ to form an oil-in-water microemulsion system. DMF (60 μL) solution containing TPA-BODIPY-OH (10 mM) was dropped into the mixture. After sonicating for 3 min, 0.2 mL VTES was added and the reaction mixture was stirred for 8 h. APTES (20 μL) was added and the mixture was further stirred at room temperature for 24 h. After the formation of nanoparticles, the unreacted starting materials were removed by dialyzing the solution against deionized water in an 8-14 kDa cutoff cellulose membrane for 72 h. The dialyzed solution was then stored at 5 ℃ for later use.

Acknowledgements

This work was financially supported by the Fundamental Research Funds for the National Natural Science Foundation of China (No. 61178057).

Notes and references

1 C. Cantürk, M. Üçüncü, and M. Emrullahoğlu, *RSC Adv.,* 2015, 5, 30522.
2 H.-r. Cheng and Y. Qian, *RSC Adv.,* 2015, 5, 82887.
3 R. R. Avirah, K. Jyothish, and D. Ramaiah, *J Org Chem,* 2008, 73, 274.

View Article Online
DOI: 10.1039/C6TB02469F

4 J. M. Baumes, J. J. Gassensmith, J. Giblin, J. J. Lee, A. G. White, W. J. Culligan, W. M. Leevy, M. Kuno, and B. D. Smith, *Nat Chem,* 2010, 2, 1025.
5 J. Frangioni, *Current Opinion in Chemical Biology,* 2003, 7, 626.
6 D. Maity, A. Raj, D. Karthigeyan, T. K. Kundu, and T. Govindaraju, *Supramolecular Chemistry,* 2015, 27, 589.
7 B. A. Smith, W. J. Akers, W. M. Leevy, A. J. Lampkins, S. Xiao, W. Wolter, M. A. Suckow, S. Achilefu, and B. D. Smith, *J Am Chem Soc,* 2010, 132, 67.
8 J. Tao, P. Zhao, and Q. Zeng, *J. Mater. Chem. B,* 2016, 4, 4258.
9 S. Chen, P. Hou, B. Zhou, X. Song, J. Wu, H. Zhang, and J. W. Foleyet, *RSC Advances,* 2013, 3, 11543.
10 L. Yuan, W. Lin, K. Zheng, L. He, and W. Huang, *Chem Soc Rev,* 2013, 42, 622.
11 A. Coskun, M. D. Yilmaz, and E. U. Akkaya, *Org Lett,* 2007, 9, 607.
12 E. Deniz, G. C. Isbasar, O. A. Bozdemir, L. T. Yildirim, A. Siemiarczuk, and E. U. Akkaya, *Org Lett,* 2008, 10, 3401.
13 Y. Hiruta, H. Koiso, H. Ozawa, H. Sato, K. Hamada, S. Yabushita, D. Citterio, and K. Suzuki, *Org Lett,* 2015, 17, 3022.
14 T. Myochin, K. Kiyose, K. Hanaoka, H. Kojima, T. Terai, and T. Nagano, *J Am Chem Soc,* 2011, 133, 3401.
15 H. Lu, J. Mack, Y. Yang, and Z. Shen, *Chem Soc Rev,* 2014, 43, 4778.
16 Y. Ni and J. Wu, *Org Biomol Chem,* 2014, 12, 3774.
17 G. Ulrich, R. Ziessel, and A. Harriman, *Angew Chem Int Ed Engl,* 2008, 47, 1184.
18 J. Banuelos, *Chem Rec,* 2016, 16, 335.
19 N. Boens, V. Leen, and W. Dehaen, *Chem Soc Rev,* 2012, 41, 1130.
20 T. Kowada, H. Maeda, and K. Kikuchi, *Chem Soc Rev,* 2015, 44, 4953.
21 X. Qian, Y. Xiao, Y. Xu, X. Guo, J. Qian, and W. Zhu, *Chem Commun (Camb),* 2010, 46, 6418.
22 H. Sunahara, Y. Urano, H. Kojima, and T. Nagano, *J Am Chem Soc,* 2007, 129, 5597.
23 A. B. Descalzo, H. J. Xu, Z. Shen, and K. Rurack, *Ann N Y Acad Sci,* 2008, 1130, 164.
24 S. Rihn, M. Erdem, A. De Nicola, P. Retailleau, and R. Ziessel, *Org Lett,* 2011, 13, 1916.
25 D. Zhang, Y. Wen, Y. Xiao, G. Yu, Y. Liu, and X. Qian, *Chem Commun (Camb),* 2008, 4777.
26 T. Bura, D. Hablot, and R. Ziessel, *Tetrahedron Letters,* 2011, 52, 2370.
27 O. Buyukcakir, O. A. Bozdemir, S. Kolemen, S. Erbas, and E. U. Akkaya, *Org Lett,* 2009, 11, 4644.
28 J. Liao, Y. Wang, Y. Xu, H. Zhao, X. Xiao, and X. Yang, *Tetrahedron,* 2015, 71, 5078.
29 T. K. Khan, S. K. Jana, M. R. Rao, M. S. Shaikh, and M. Ravikanth, *Inorganica Chimica Acta,* 2012, 383, 257.
30 A. Poirel, A. De Nicola, and R. Ziessel, *Org Lett,* 2012, 14, 5696.
31 L. N. Sobenina, O. V. Petrova, K. B. Petrushenko, I. A. Ushakov, A. I. Mikhaleva, R. Meallet-Renault, and B. A. Trofimov, *European Journal of Organic Chemistry,* 2013, 2013, 4107.
32 M. Ren, B. Deng, J.-Y. Wang, Z.-R. Liu, and W. Lin, *J. Mater. Chem. B,* 2015, 3, 6746.
33 L. Wang, J. Yan, W. Qin, W. Liu, and R. Wang, *Dyes and Pigments,* 2012, 92, 1083.
34 X. Zeng, L. Dong, C. Wu, L. Mu, S.-F. Xue, and Z. Tao, *Sensors and Actuators B: Chemical,* 2009, 141, 506.
35 Y. Zhao, B. Zheng, J. Du, D. Xiao, and L. Yang, *Talanta,* 2011, 85, 2194.
36 M. Vedamalai and S.-P. Wu, *European Journal of Organic Chemistry,* 2012, 2012, 1158.
37 A. Atkinson and D. R. Winge, *Chem Rev,* 2009, 109, 4708.
38 D. Galaris, V. Skiada, and A. Barbouti, *Cancer Lett,* 2008, 266, 21.
39 C. D. Kaplan and J. Kaplan, *Chem Rev,* 2009, 109, 4536.
40 E. C. Theil and D. J. Goss, *Chem Rev,* 2009, 109, 4568.
41 K. Liu, Z. Xu, M. Yin, W. Yang, B. He, W. Wei, and J. Shen, *Journal of Materials Chemistry B,* 2014, 2, 2093.
42 K. B. Li, H. Wang, Y. Zang, X. P. He, J. Li, G. R. Chen, and H. Tian, *ACS Appl Mater Interfaces,* 2014, 6, 19600.
43 Z. Xu, J. Yoon, and D. R. Spring, *Chemical Communications,* 2010, 46, 2563.
44 H.-r. Cheng and Y. Qian, *Sensors and Actuators B: Chemical,* 2015, 219, 57.
45 H.-r. Cheng, Y. Qian, Y. Yang, and H.-l. Liu, *RSC Adv.,* 2015, 5, 86371.
46 J. V. Cooney, E. J. Beal, and R. N. Hazlett, *Organic Preparations and Procedures International,* 2009, 15, 292.
47 H.-r. Cheng and Y. Qian, *Dyes and Pigments,* 2015, 112, 317.
48 M. Baruah, W. Qin, R. A. Vallee, D. Beljonne, T. Rohand, W. Dehaen, and N. Boens, *Org Lett,* 2005, 7, 4377.
49 M. Chen, X. Lv, Y. Liu, Y. Zhao, J. Liu, P. Wang, and W. Guo, *Org Biomol Chem,* 2011, 9, 2345.
50 L. Wang, G. Fang, and D. Cao, *Sensors and Actuators B: Chemical,* 2015, 207, 849-857.
51 C. Li, T. Bai, F. Li, L. Wang, X. Wu, L. Yuan, Z. Shi and S. Feng, *CrystEngComm,* 2013, 15, 597-603.
52 C. Li, Y. Zhao, F. Li, Z. Shi, and S. Feng, *Chemistry of Materials,* 2010, 22, 1901-1907.
53 F. Li, C. Li, J. Liu, X. Liu, L. Zhao, T. Bai, Q. Yuan, X. Kong, Y. Han, Z. Shi and S. Feng, *Nanoscale,* 2013, 5, 6950-6959.
54 F. Li, C. Li, X. Liu, Y. Chen, T. Bai, L. Wang, Z. Shi and and S. Feng, *Chemistry,* 2012, 18, 11641-11646.